07

Power Source based on $Al_{0.8}Ga_{0.2}As/GaAs$ photovoltaic converter and $YPO_4:Eu/(^{238}Pu)$ radioluminescent emitter

© K.K. Prudchenko, I.A. Tolkachev, E.V. Kontrosh, E.A. Silantieva, V.S. Kalinovskii

Ioffe Institute,
194021 St. Petersburg, Russia
e-mail: prudchenkokk@mail.ioffe.ru

Received August 8, 2022
Revised September 23, 2022
Accepted September 24, 2022

An AlGaAs/GaAs photovoltaic converter for a mock-up of an environmentally friendly radioisotope energy source of ultra-long use with a $YPO_4:Eu/(^{238}Pu)$ radioluminescent emitter with an extremely low content of the isotope $^{238}Pu < 0.1$ wt.% was studied. The modeling of the $Al_{0.8}Ga_{0.2}As/GaAs$ heterostructure for the conversion of nanowatt power levels of an optical signal has been carried out. The calculated and experimental efficiency of the mock-up with a photovoltaic converter at a radioluminescent source power of 1 nW was $\sim 1.4\%$.

Keywords: radioisotope energy source, AlGaAs/GaAs photo converter, optical radiation radioluminescent source, current flow mechanisms, conversion efficiency.

DOI: 10.21883/TP.2022.12.55199.199-22

Introduction

In various fields of modern technology and nanoelectronics there is a need for low-current, with an extra long service life electric power sources. In this regard, much attention is paid to the development and improvement of radioisotope energy sources (RES), in which the energy of radioactive decay of isotopes is converted into electrical energy [1–4]. Such energy sources can be used in nanoelectronics, medicine, instrumentation, in complicated hard-to-reach or aggressive environments, nuclear and chemical industries. The period of use of such sources is determined by the half-life of the radionuclide, for ^{238}Pu it is 87 years.

Currently, there are energy sources based on the radioactive decay of radionuclides. These, first of all, include radioisotope thermoelectric generators (RiTEG). They have large overall dimensions, a high content of isotopes, which leads to their limited use and radiation insecurity. There are devices based on the beta-voltaic effect, when the energy of β-radiation is directly converted into electrical energy in the active region of a semiconductor element [5,6]. Such power sources, as a rule, are made on the basis of such isotopes as tritium ^3H, nickel ^{63}Ni, carbon ^{14}C, etc. RES with direct conversion of radioactive decay energy into electricity, as a rule, due to the destructive effect of ionizing radiation directly on the devices powered by them, they require additional protection against radiation and have a much shorter service life, unlike RES with double conversion. In radioisotope photovoltaic generators (RiPvG), the decay energy of isotopes is converted into optical radiation, and then into electricity using photovoltaic converters (PVCs). RiPvG devices have a lower level of electrical energy at output, but also significantly smaller dimensions, higher reliability, safety and longer service life. In general, such devices can achieve a conversion efficiency more than 5% [7]. At the same time, RiPvG with photocells converting optical radiation stimulated by β-radiation [6,7] are, as a rule, less efficient in comparison with power supplies with α-radiating base. Due to the fact that α-particles are have much higher energy, the difference in the specific power of ionizing radiation is significant and, as a result, the efficiency of photovoltaic conversion is higher.

Radiation-resistant mineral-like matrices, for example, crystals of the YPO_4 xenotime type, doped with the radionuclide $^{238}Pu \leq 0.1$ wt.% and with europium ions $Eu^{3+} \sim 2-3$ wt.% [8] are the optical source in RiPvG. It is also possible to use other similar radioluminescent sources based on crystals of zirconium orthosilicate $ZrSiO_4$: (Tb^{3+} — 0.2 wt.%), (^{238}Pu — 0.02 wt.%), ceramics based on polycrystalline cubic zirconium ZrO_2: (Eu^{3+} — 9.4 wt.%), (Tb^{3+} — 1.3 wt.%), (^{238}Pu — 0.3 wt.%) [9]. Many studies were carried out to study the radiation resistance of these radioluminescent sources [10]. The use of highly efficient nanoheterostructural AlGaAs/GaAs PVC and safe radioluminescent sources makes it possible to ensure the maximum RES capacity for a long time, on the order of the half-life of an isotope. Taking into account the almost complete absence of radiation exposure, the proposed AlGaAs/GaAs PVC, thus, has a service life typical for photodetectors and solar cells (SC) based on GaAs. The purpose of this paper is to develop a structure based on AlGaAs/GaAs PVCs and study its characteristics with an assessment of the effectiveness of its use in RiPvG prototype.

1. Simulation

The dependence of the optical radiation absorption in p-GaAs [11] is calculated for the wavelengths correspond-

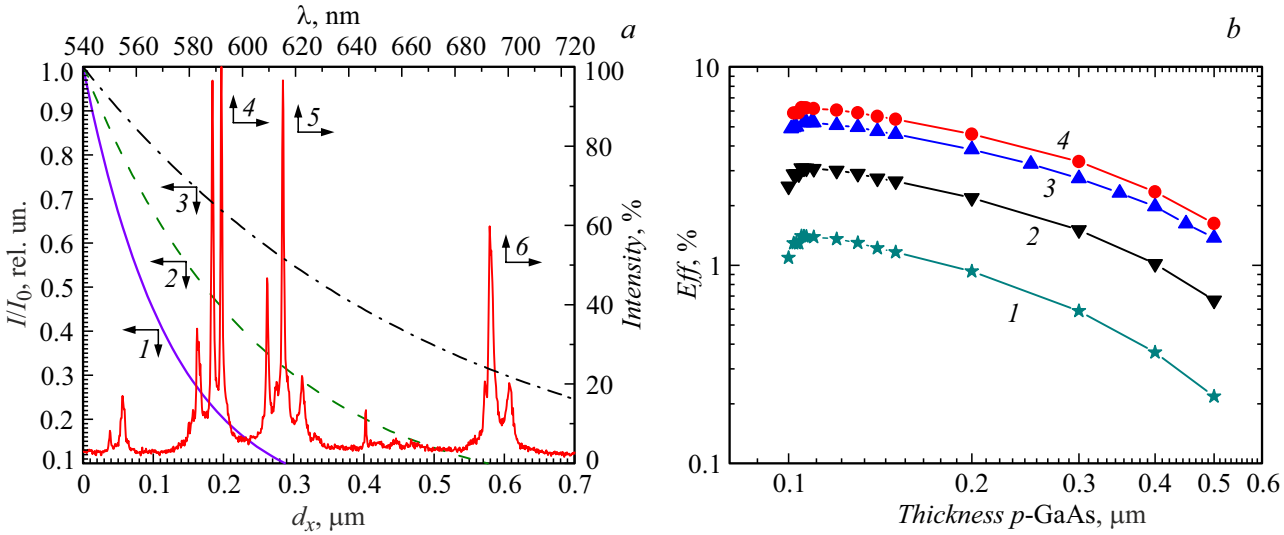

Figure 1. *a* — calculated absorption curves (*1–3*) in *p*-GaAs of luminescent radiation of radioisotope source $YPO_4:Eu/(^{238}Pu)$ at wavelengths $\lambda_1 = 595$ nm (*4*), $\lambda_2 = 615$ nm (*5*) , $\lambda_3 = 695$ nm (*6*) respectively; *b* — calculated dependences of the efficiency on the thickness of the emitter *p*-layer in the GaAs *p*–*n*-junction of the PVC when excited by optical radiation ($\lambda_1 = 595$ nm) with powers: *1* — 1, *2* — 10, *3* — 50, *4* — 100 nW.

ing to the maxima of the intensity peaks in the spectrum of the radioluminescent source $YPO_4:Eu/(^{238}Pu)$ [9]. The calculations were carried out with dopant concentrations $N_D = 5 \cdot 10^{17}\,cm^{-3}$ and absorption coefficients $k_1 = 8 \cdot 10^4\,cm^{-1}$ ($\lambda_1 = 595$ nm); $k_2 = 4 \cdot 10^4\,cm^{-1}$ ($\lambda_2 = 615$ nm); $k_3 = 2 \cdot 10^4\,cm^{-1}$ ($\lambda_3 = 695$ nm) [12].

From the calculated curves (Fig. 1, *a*), where the arrows indicate their corresponding axes, it can be seen that the depth of light absorption at the selected wavelengths is in the range of $0.15-0.5\,\mu$m. Considering that the peak of the optical radiation of the radioisotope source $YPO_4:Eu/(^{238}Pu)$ with the maximum intensity and energy corresponds to the wavelength $\lambda_1 = 595$ nm, we consider ($\lambda_1 = 595$ nm (Fig. 1, *a*)).

The software package simulated the $Al_{0.8}Ga_{0.2}As/GaAs$ PVC structure optimized for a radioluminescent source of optical radiation of nanowatt power based on a mineral-like crystal xenotime $YPO_4:Eu/(^{238}Pu)$, and its J-U characteristics. The criteria for evaluating the optimality of the AlGaAs/GaAs PVC structure, which converts ultra-low subnanowatt power levels of the optical radiation source, were the depth of *p*–*n*-junction, the thickness of the *p*-layer, the doping levels, and as a result — the conversion efficiency of line spectrum of radioluminescent source. The structure was simulated in the following configuration (from top to bottom): subcontact layer (*p*-GaAs, $N_A = 4 \cdot 10^{18}\,cm^{-3}$) $h = 300$ nm thick, wide-gap window (*p*-$Al_{0.8}Ga_{0.2}As$, $N_A = 7 \cdot 10^{17}\,cm^{-3}$), $h = 35$ nm; *p*–*n* transition from *p*-GaAs, $N_A = 7 \cdot 10^{17}\,cm^{-3}$ and *next*–GaAs, $N_D = 1 \cdot 10^{17}\,cm^{-3}$ with thicknesses of *p* and *n*-layers 100 nm and $3\,\mu$m respectively; back barrier (*n*-$Al_{0.2}Ga_{0.8}As$, $N_D = 3 \cdot 10^{18}\,cm^{-3}$), $h = 50$ nm and buffer layer (*n*-GaAs, $N_D = 5 \cdot 10^{18}\,cm^{-3}$), $h = 200$ nm on *n*-GaAs substrate, $N_D = 2 \cdot 10^{18}\,cm^{-3}$ thick $h = 350\,\mu$m. The radiation spectrum was set as close as possible to the spectrum of the radioluminescent source $YPO_4:Eu/(^{238}Pu)$.

It can be seen from the calculations presented in Fig. 1, *b* that at thicknesses of the *p*-layer less than 105 nm, the increase in the efficiency of the simulated PVC is observed, then at the optimal thickness of *p*-layer ~ 105 nm, the efficiency value reaches a maximum and then decreases with *p*-layer increasing.

2. Experiment

2.1. Materials and methods

Two AlGaAs/GaAs heterostructures were used to carry out experimental studies and evaluate the performed calculations (Table 1). One was obtained by molecular beam epitaxy (MBE) and coinciding with the simulated one, where beryllium (Be) was used as an acceptor impurity, and silicon (Si) as a donor impurity.

The second structure of the AlGaAs/GaAs PVC, obtained by liquid-phase epitaxy (LPE), contains a subcontact layer *p*-GaAs:Zn, $N_A \geq 5 \cdot 10^{18}\,cm^{-3}$ $h \geq 500$ nm thick, wide-gap window *p*-$Al_{0.8}Ga_{0.2}As$:Zn, $N_A = 3 \cdot 10^{18}\,cm^{-3}$ $h < 2000$ nm thick, then *p*-layer GaAs $h < 1500$ nm thick (*p*-GaAs:Zn, $N_A = 3 \cdot 10^{18}\,cm^{-3}$) and *n*-GaAs:Sn with a base $h = 20\,\mu$m thick (GaAs:Sn, $N_D = 1 \cdot 10^{17}\,cm^{-3}$) on an *n*-GaAs:Sn substrate, ($N_D = 1 \cdot 10^{18}\,cm^{-3}$), $h = 350\,\mu$m. This structure was used taking into account the fact that the LPE method can grow a high-quality *p*–*n*junction in GaAs, with low „saturation“ currents for the tunnel-trap, „excess“ and recombination mechanisms of

Table 1. Composition and thicknesses of heterostructure layers

Number of layer	Thickness of layer, nm	Composition	Concentration of impurity, cm^{-3}
MBE method			
1	300	GaAs:Be	$4 \cdot 10^{18}$
2	35	$Al_{0.8}Ga_{0.2}As$:Be	$7 \cdot 10^{17}$
3	100	GaAs:Be	$7 \cdot 10^{17}$
4	3000	GaAs:Si	$1 \cdot 10^{17}$
5	50	$Al_{0.2}Ga_{0.8}As$:Si	$3 \cdot 10^{18}$
6	200	GaAs:Si	$5 \cdot 10^{18}$
7	35 0000	GaAs:Si	$2 \cdot 10^{18}$
LPE method			
1	1000	$Al_{0.8}Ga_{0.2}As$:Zn	$5 \cdot 10^{18}$
2	1500	GaAs:Zn	$3 \cdot 10^{18}$
3	20 000	GaAs:Sn	$1 \cdot 10^{17}$
4	35 0000	GaAs:Sn	$1 \cdot 10^{18}$

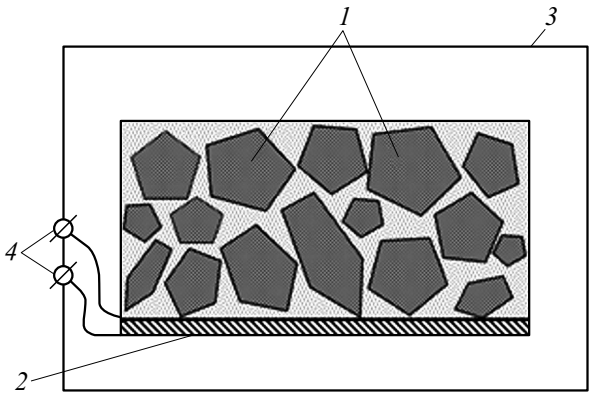

Figure 2. Schematic representation of RiPvG based on the developed AlGaAs/GaAs photoconverter and YPO_4:Eu/(^{238}Pu) radioluminescent radiation source: *1* — matrix with radioluminescent crystals, *2* — AlGaAs/GaAs photoconverter, *3* — protective housing, *4* — external electrical contacts.

current flow, which is important when converting weak, nanowatt optical signals.

Samples of MBE and LPE structures with multilayer contact with surface metallization with gold, 3×3 mm and 2×2 mm, respectively, were studied in the experiments.

To evaluate the effectiveness of the RiPvG prototype being created (Fig. 2), measurements of the spectral sensitivities, dark and light J-U characteristicss of PVCs of these types of structures were performed. Characteristics are shown in Fig. 3, 4. Note that in order to increase the efficiency of the AlGaAs/GaAs prototype PVCs can be placed on both sides of the source of optical radiation [13]. The dependences of the external quantum efficiency of PVC on the wavelength in the range of 400−890 nm were made on unit based on a monochromator (M266) with a halogen lamp as a radiation source. Measurements of PVC J-U characteristics and the RiPvG prototype were carried out at the probe station using a high-precision source —meter (Keithley 2635A), which allows measurements in the current range 10 pA (0.15% + 120 fA) — 1.5 A (0.05% + 3.5 mA). The power level of the optical radiation source was monitored by an optical power meter with a calibrated silicon photodetector with a spectral sensitivity in the range of (400−1100) nm and a minimum measured power level of 20 pW.

2.2. Results

To analyze the experimental dark J-U characteristics we used the method described in [14]. The method is based on the representation of the direct branch of the dark J-U characteristics, consisting of three exponential sections corresponding to the tunnel-trap („excess"), recombination and diffusion mechanisms of current flow, described by expression (1):

$$J = J_{0t}\left(\exp(qV_j/A_tkT) - 1\right) + J_{0r}\left(\exp(qV_j/A_rkT) - 1\right) + J_{0d}\left(\exp(qV_j/A_dkT) - 1\right), \quad (1)$$

where $qV_j = (F_n - F_p)$ is the difference between the electron and hole Fermi quasi-levels at the boundaries of the space charge region (SCR) of the $p-n$-transition. Accordingly, V_j — the so-called resistanceless voltage, independent of the series resistance of the structure R_S, $V_j = V - JR_S$, where V — voltage across the entire $p-n$-structure. $A_t > 2$, $A_r = 2$, $A_d = 1$ — corresponding diode coefficients.

From the fitting of the experimental dark J-U characteristics according to the three-exponential prototype (Fig. 3, *a*) and the literature [14,15] it follows that the prevailing current flow mechanisms in the SCR of the GaAs PVC when converting weak nanowatt levels the power of the optical radiation of the source is tunnel-trap („excess") and recombination.

In our case, the „saturation" currents of the tunnel-trap, recombination, and diffusion mechanisms of current flow for the PVC structure grown by the MBE were

$$J_{0t} = 3.4 \cdot 10^{-10}\ \text{A/cm}^2,\ J_{0r} = 2 \cdot 10^{-11}\ \text{A/cm}^2,$$

$$J_{0d} = 2.4 \times 10^{-20}\ \text{A/cm}^2,$$

which is somewhat lower than the corresponding values obtained for the PVC structure grown by LPE:

$$J_{0t}=3.6 \cdot 10^{-9}\ \text{A/cm}^2,\ J_{0r}=6 \cdot 10^{-11}\ \text{A/cm}^2,$$

$$J_{0d} = 8.6 \cdot 10^{-19}\ \text{A/cm}^2.$$

From the spectral dependences shown in Fig. 3, *b*, it can be seen that the PVC structure obtained by MBE and

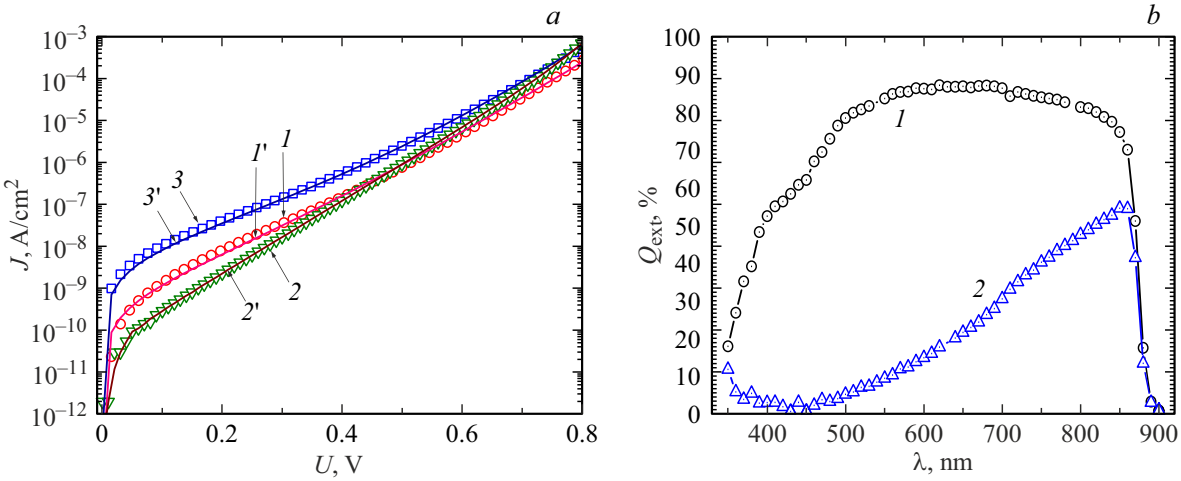

Figure 3. *a* — direct „dark" J-U characteristics of AlGaAs/GaAs PVC. MBE structure: experiment (*1*) simulated in Silvaco (*2*); LPE structure: experiment (*3*), *1′–3′* — corresponding calculated curves (by formula (1) bf); *b* — spectral characteristics of the external quantum efficiency of $Al_{0.8}Ga_{0.2}As/GaAs$ PVC: *1* — MBE structure, *2* — structure LPE.

Table 2. Parameters determined from the fitting of experimental and simulated dark and light J-U characteristicss of PVC grown by MBE and LPE methods

Structure	A_t	J_{0t}, A/cm^2	A_r	J_{0r}, A/cm^2	A_d	J_{0d}, A/cm^2	R_s, Ω · cm^2	$I^*_{\text{sh .cir.}}$, pA	U^{**}_{idle}, V	P^{***}_{max}, pW	FF^{****}, %	Efficiency, %
MBE (experiment)	> 2	$3.4 \cdot 10^{-10}$	2	$2 \cdot 10^{-11}$	1	$2.4 \cdot 10^{-20}$	2.6	175	0.18	16.5	52	1.4
MBE (simulation)	> 2	$1.9 \cdot 10^{-11}$	2	$2.2 \cdot 10^{-11}$	1	$1.9 \cdot 10^{-20}$	0.002	163	0.17	16	58	1.38
LPE (experiment)	> 2	$3.6 \cdot 10^{-9}$	2	$6 \cdot 10^{-11}$	1	$8.6 \cdot 10^{-19}$	0.05	40	0.17	4.7	72	0.3

Note. * — short circuit current, ** — open circuit voltage, *** — power at optimum load point, **** — fill factor of the load characteristic.

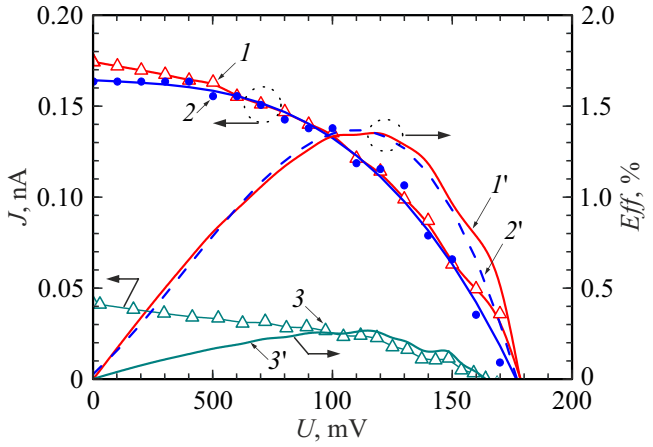

Figure 4. Experimental (*1, 3*) and simulated (*2*) light J-U characteristicss; calculated from the experimental J-U characteristics (*1′*, *3′*), and simulated (*2′*) dependences of the efficiency for the studied PVC structures when excited by luminescent radiation from radioisotope source $YPO_4:Eu/(^{238}Pu)$ with power 1 nW (curves *1*, *1′*, *2*, *2′* — MBE structure, curves *3*, *3′* — LPE structure).

close to the mathematically simulated (optimized) has a significantly higher sensitivity than the structure grown by the LPE method, in the range of optical radiation of interest to us.

The power of the luminescent radiation of the radioisotope $YPO_4:Eu/(^{238}Pu)$ source at wavelengths $\lambda_{1-3} = (595, 615, 695)$ nm (Fig. 1, *a*) used in the RiPvG prototype was $P_{\text{opt}} = 1$ nW. It follows from Fig. 4 and Table 2 that for the prototype RiPvG with the developed $Al_{0.8}Ga_{0.2}As/GaAs$ PVC (MBE), the efficiency value is 1.4%, and with PVC (LPE) with non-optimized structure — < 0.3%.

For PVCs from structures grown by the MBE and LPE methods, there is a good agreement between the efficiency values obtained by simulation and from measurements at an optical radiation power of 1 nW (Fig. 5).

Note that for the parameters of PVC structures used in the calculations the efficiency depends both on the power of the incident radiation and on the magnitudes of the „saturation" currents of the prevailing current flow mechanisms. For example, at an optical power of ∼ 100 nW for $Al_{0.8}Ga_{0.2}As/GaAs$ PVC (MBE), the efficiency increases to 6%, (Fig. 5, curve *1*).

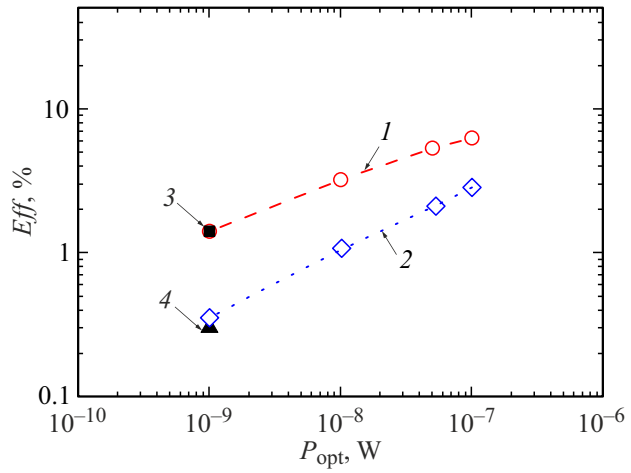

Figure 5. Simulated dependences of the efficiency (curves *1, 2*) on the power of the incident optical radiation and experimentally obtained efficiency values (dots *3, 4*) for $Al_{0.8}Ga_{0.2}As/GaAs$ PECs grown by MBE and LPE technologies, respectively, at incident optical power $P_{opt} = 1$ nW.

Conclusion

The possibility is shown of using AlGaAs/GaAs PVC in safe, environmentally friendly, long-term radioisotope photovoltaic power sources with a radioluminescent emitter based on $YPO_4:Eu/(^{238}Pu)$.

The AlGaAs/GaAs PVC obtained by the MBE method at an optical radiation level of 1 nW ensured the efficiency of $\sim 1.4\%$ in the RiPvG prototype. The obtained experimental value of the efficiency is in good agreement with the results of simulation and the efficiency calculations of AlGaAs/GaAs PVC. As the calculations show, with increase in the optical power of radioluminescent radiation sources based on $YPO_4:Eu/(^{238}Pu)$, it is possible to provide the output electric power level of up to 0.2 mW and more during the half-life of the isotope impregnated into the xenotime matrix.

Acknowledgment

The authors express their gratitude to V.I. Khvostikov for providing samples of PVC structures for experiments.

Conflict of interest

The authors declare that they have no conflict of interest.

References

[1] O.L. Ayodele, K.O. Sanusi, M.T. Kahn. J. Engineering, Design and Technology, **17** (1), 172 (2019). DOI: 10.1108/JEDT-02-2017-0011
[2] Z. Xu, Yu. Liu, Zh. Zhang, W. Chen, Z. Yuan, K. Liu, X. Tang. Wiley Energy Research, **42** (4), 1729 (2018). DOI: 10.1002/er.3982
[3] A.A. Krasnov, S.A. Legotin. Instruments and Experimental Techniques, **63** (4), 437 (2020).
[4] Zh.-R. Zhang, X.-B. Tang, Yu.-P. Liu, Zh.-H. Xu, Z.-Ch. Yuan, K. Liu, W. Chen. Nuclear Instruments and Methods in Physics Research B, **398**, 35 (2017). DOI: 10.1016/j.nimb.2017.03.060
[5] A.A. Svintsov, E.B. Yakimov, M.V. Dorokhin, P.B. Demina, Yu.M. Kuznetsov. Semiconductors, **53** (1), 96 (2019).
[6] S. Deus. Proc. 28 st IEEE Photovoltaics Specialist Conf., 1246–1249 (2000).
[7] V.V. Svetukhin, S.G. Novikov, A.V. Berintsev, A.A. Chertoriysky, A.S. Alekseev. Proceedings of Universities. Electronics, **21** (5), 429 (2016).
[8] B.E. Burakov, V.M. Garbuzov, A.A. Kitsay, V.A. Zirlin, M.A. Petrova, Ya.V. Domracheva, M.V. Zamoryanskaya, E.V. Kolesnikova, M.A. Yagovkina, M.P. Orlova. Semiconductors, **41** (4), 427 (2007). DOI: http://dx.doi.org/10.1134/S1063782607040124
[9] M.V. Zamoryanskaya, E.V. Dementeva, K.N. Orekhova, V.A. Kravets, A.N. Trofimov, G.A. Gusev, I. Ipatova, B.E. Burakov. Materials Research Bulletin, **142**, 111431 (2021). DOI: 10.1016/j.materresbull.2021.111431
[10] B.E. Burakov, M.I. Ojovan, W.E. Lee (Ed.). *Crystalline Materials for Actinide Immobilization, 1* (Imperial College Press, 2010)
[11] B. Wardle. *Principles and Applications of Photochemistry* (Wiley, 2010), p. 30.
[12] S.M. Sze. *Physics of Semiconductor Devices* (John Wiley & Sons, NY., Chichester, Brisbar, Toronto, Singapore, 1981)
[13] K.K. Prudchenko, M.V. Zamoryanskaya, V.S. Kalinovskii, E.V. Kontrosh, I.A. Tolkachev, K.N. Orekhova, A.N. Trofimov, B.E. Burakov, E.V. Dement'eva. Radioizotopny istochnik energii, Patent RF №RU 207 579 (02.11.2021) (in Russian)
[14] V.M. Andreev, V.V. Evstropov, V.S. Kalinovsky, V.M. Lantratov, V.P. Khvostikov. Semiconductors, **43** (5), 644 (2009). DOI: 10.1134/S1063782609050200
[15] V.S. Kalinovskii, E.V. Kontrosh, G.V. Klimko, T.S. Tabarov, S.V. Ivanov, V.M. Andreev. Tech. Phys. Lett., **44** (11), 1013 (2018). DOI: 10.1134/S1063785018110214